Journal Article

Forced air cooled heat sink with uniformly distributed temperature of power electronic modules

Bünnagel, C., Monir, S., Sharp, A., Anuchin, A., Durieux, O., Uria, I. and Vagapov, Y.

Forced Air Cooled Heat Sink with Uniformly Distributed Temperature of Power Electronic Modules

Christian Bünnagel[a], Shafiul Monir[a], Andrew Sharp[a], Alecksey Anuchin[b], Olivier Durieux[a], Ikea Uria[a], Yuriy Vagapov[a]*

[a] Faculty of Art, Science and Technology, Glyndwr University, Mold Road, Wrexham, LL11 2AW, UK

[b] Department of Electric Drives, Moscow Power Engineering Institute, 14 Krasnokazarmennaya Street, Moscow, 111250, Russia

* Corresponding author: tel.: +44(0)1978 293392; e-mail: y.vagapov@glyndwr.ac.uk

Highlights:

- Low-cost improvement of conventional heat sink for power electronic modules
- Redistribution of the airflow through the heat sink fins using V-cut guide plate
- Uniform distribution of the temperature across the power electronic modules
- Modelling and verification of the proposed power semiconductor cooling system

Abstract

The paper discusses an approach to the design of the forced air-cooling heat sink for power electronic application to uniformly distribute the temperature of the semiconductor modules fixed on the top of the heat sink. The proposed approach suggests a minor modification of a conventional fin-based heat sink commonly manufactured for cooling of power electronic modules. Following the proposed modification, an air guide plate having a V-shaped cut is attached to the bottom of the heat sink to redistribute the airflow through the fins. To verify the proposed approach, the modified forced air-cooling system for a power electronic circuit comprising of three IGBT modules was modelled and numerically simulated using Ansys Fluent software under steady-state conditions. The numerical analysis was conducted for a range of power loss 50-100W in each IGBT module and an airspeed of 5 m/s through the heat sink. The simulation results have shown a good uniform distribution of the temperature across the IGBT modules where the temperature difference does not exceed 0.21°C.

Keywords: Power Electronics, Heat Sink, Forced Air Cooling; Uniform Temperature Distribution, Air Guide Plate, Semiconductor Reliability, Semiconductor Lifetime

1. Introduction

Over the last decade, the area of applications of power electronics systems has significantly expanded. Nowadays, it is intensively used in a large variety of domestic, industrial, transportation and energy applications. Due to the enhanced integration of power electronics in various engineering systems, the power electronic elements and units have become crucial components in terms of system reliability and operational lifetime. Extended demand for safe and reliable system operation requires the implementation of advanced and comprehensive approaches to the development and design of new power electronic devices [1].

Demanding applications of power electronics, practically in the area of vehicles and aircraft propulsion, are characterised by a system high-power density where power electronics is operating under substantial thermal stress factors. These factors are related to (1) the ambient temperature which can be quite high due to compact and air isolated system enclosure and (2) the power loss in the semiconductor devices following the power cycling according to a mission profile. Semiconductor devices are sensitive to the junction temperature and failure of a power electronic unit can occur by component overheat. Therefore, the efficiency of the cooling system applied to the power semiconductors significantly determines the device reliability and operation lifetime [2]. According to the report by Yang *et al*. [3], the most prone to failure components in power electronic converters are power semiconductors and constitute 31% of all component failures.

Despite improvement in the efficiency rate, the power semiconductors are still responsible for a significant amount of heat generated in the junction by power loss (up to 1kW for high power applications). A very common solution for thermal management of power semiconductors is a heat sink which provides dissipation of power loss produced in the junction into an ambient. Heat sinks are core components of natural and forced convection air-cooling systems widely used in industrial applications and considered as the most cost-effective solution [4].

A typical installation of power semiconductor modules in 3-phase applications is a circuitry combination of 3 or 6 modules attached on the top of a rectangular heat-sink in one row with forced airflow through the heat-sink fins. Many standard heat sinks are designed and produced for this purpose by industrial manufactures for a large range of power electronic converters for ac electric drives, 3-phase power supplies, uninterruptable power

sources etc. The disadvantage of such installation is the different temperatures of the power electronic components. The device located close to the air inlet is cooled better than the device attached to the opposite end of the heat sink (outlet). In general, this is related to the increase of the temperature of airflow through the heat sink. The cold air at the heat sink inlet provides the best cooling condition for the first power semiconductor device. The further increase in the airflow temperature deteriorates the cooling conditions for the second and third devices installed in the middle and at the heat sink outlet. Therefore, the temperature of the semiconductors is increased in the direction of airflow. The third semiconductor device installed close to the airflow outlet has the highest temperature and determines the system reliability as the most thermally loaded component.

The temperature difference across the heat sink produces the temperature gradient in the semiconductor structures and affects the mechanical stress development in the module package. Modern semiconductor modules for power electronic applications have a large surface area of the semiconductor structure. Such a large area is very sensitive to the temperature gradient stress produced by the non-uniform temperature distribution. It has been reported [5] that the mechanical stress occurred inside the semiconductor structure significantly impacts the power electronic device lifetime and reliability. The temperature difference also causes the difference in the temperature-dependent parameters of power semiconductors such as leakage current, saturation voltage, switching time. In some applications, this difference might affect the performance of the external electrical/electronic circuit and power loss produced in the semiconductors.

The most advanced methods to uniform the temperature across the semiconductor modules installed in one row on the top of the heat sink are based on active thermal control techniques. Usually, an active thermal technique is implemented to control a semiconductor temperature using power loss adjustment where typical control parameters are switching frequency and duty cycle of the pulse width modulation of a heat-generating device [6]. Following the active thermal technique applied for the row of semiconductor modules, the controller provides operation of the power semiconductors in a way to redistribute power loss (in general, the conduction and switching losses) between the power semiconductors. The power loss is reduced in the semiconductors having the highest temperature and vice versa to uniformly adjust the temperature in the semiconductor junctions. For example, redistribution of power loss in the power semiconductor modules of the 3-phase inverter for switched reluctance drive using model predictive control and the cost function algorithm is suggested

in [7]. Installation of semiconductor modules in a particular order on the heat sink operating under active thermal control is proposed in [8] to uniform temperature across the devices.

The benefit of active thermal control is that this option is suitable for a conventional forced air-cooling system built on a standard heat sink. It does not require any modification of mechanical components or design of the cooling system as the active thermal management method is implemented into the control algorithm at a software level. However, the loss redistribution across the power semiconductors provided by an active thermal control is not an optimal solution in terms of device operational efficiency. Implementation of this approach can often increase the total power loss in the system and is usually applied for the specific purpose to achieve the lower level of temperature variation in the power semiconductor junctions.

Special heat sink design is another relatively simple option to uniform the temperature of power electronic devices. It is applicable for both natural and forced cooling systems. Various heat sink designs are proposed to adjust the temperature for both single and multi-component heat-generating semiconductors [9]. These designs are mainly developed to ensure varying thermal resistance over the heat sink body.

There are many approaches to the heat sink design aimed to uniform the distribution of temperature across the heat sink produced by a non-uniform heat source. A very common approach is a complex geometrical structure of heat-sink reflecting a non-uniform nature of the heat source. For example, Huang and Chen [10], [11] analysing the square pin-based heat sinks for the air-cooling systems suggested increasing the “pin-density” in the areas with the higher heat generation to ensure more efficient heat transfer condition. Another approach related to the change of the heat sink fin geometry is proposed by Wang *et al*. [12] where the density of fins/channel widths is gradually increased following the increase in heat flow gradient produced by a high-power semiconductor. A heat sink having the variable height of the fins is proposed by Al-Khamaiseh *et al*. [13]. The highest fins are installed in the heat sink zone where the heat flow generation is maximum. All uniform temperature solutions based on special heat sink geometry are not applicable for the standard heat sinks produced by industry and available “on-shelf”. The non-standard and complicate design of heat sinks for uniform temperature distribution requires an advanced manufacturing process and makes the heat sink products expensive.

An interesting approach to the improvement of heat sink efficiency which does not require heat sink modification is reported by Elsayed *et al*. [14]. The report discussed the method to redistribute the forced airflow using a partial shield and guide plate. Elsayed *et al*.

[14] analysed cooling system efficiency and thermal management obtained under bypassing the airflow over the heat sink directed by shield or partial shield with a guide plate. However, this approach is not applicable for a multi-component cooling configuration to uniform the temperature across the semiconductor devices.

This paper suggests a heat sink based solution to uniform the temperature of the power semiconductor modules composed of a 3-phase converter device having a forced air-cooling system. The focus of the solution is to provide a low-cost improvement in the heat-sink design. Therefore, the proposal does not require major modification of the standard heat sinks and can be applied for the improvement of existing power electronics installations. According to the solution, a guide plate having a V-cut is attached to the opposite side of the heat sink to increase the airspeed in the heat sink end where the hottest semiconductor module is mounted. The solution was numerically analysed and investigated to verify the proposed approach.

2. Proposed Approach

A conventional forced air-cooling system usually comprises of a heat sink with an air guide plate attached to form the fins area into air channels. As mentioned above, the disadvantage of such a cooling configuration is the non-uniform distribution of the temperatures across the power semiconductors fixed on the top of the heat sink base in a row alongside the airflow. In order to reduce the temperature difference between the semiconductor devices, it is suggested to make a V-shape cut on the air guide plate. Fig. 1 illustrates the principle of the proposed improvement of the heat sink using a V-cut guide plate. The V-cut in the guide plate is the only modification that differs the proposed solution from a convention heat sink cooling system. It can be seen that the air guide plate is attached to the heat sink in a way to expand the inlet area in comparison to the conventional cooling scheme. In fact, the V-cut makes the inlet area larger than the outlet area. Due to the difference between the inlet and outlet areas the airspeed at the heat sink outlet is higher. Therefore, the convection heat transfer related to the airspeed provides better cooling conditions at the outlet area of the heat sink. It means that the power semiconductor 3, as shown in Fig. 1, has lower thermal resistance than semiconductors 1 and 2. Correspondingly, semiconductor 2 has better thermal resistance than semiconductor 1. If each semiconductor device has the same power loss, the different thermal resistances will reduce the temperature difference between the semiconductors and the uniform temperature can be achieved under a certain size of the V-cut.

The reason for the V-cut selection is related to the cost of potential implementation in the mass-production of power electronic equipment. The implementation should be applicable to standard, widely used heat-sinks at the lowest cost. It is assumed that the single V-cut of existing guide plates is the most simple and cost-efficient solution for the manufacturers. In terms of implementation cost, other cut-out shapes are considered more complicated in comparison to the proposed shape.

The proposed solution introducing the V-cut in the guide plate is applicable for a variety of standard three-phase power electronic inverters supplying induction motors, the most common type of electric drives in the industry. The principle of the solution is based on fact that the distribution of power losses across the power semiconductor modules comprising a conventional three-phase inverter is equal for each semiconductor.

Fig. 1 shows that the inlet area significantly depends on the V-cut dimensions. It means that the V-cut length determines the thermal resistances and, therefore, the temperature distribution across the power semiconductor devices. The following numerical modelling and simulation are focused to investigate how the V-cut dimensions affect the distribution of the temperatures across power modules and what is the optimum length of the V-cut to provide the uniform temperatures.

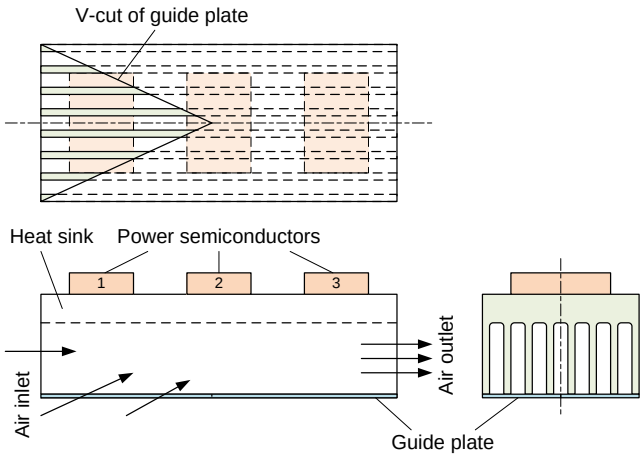

Fig.1 Illustration of the principle of the proposed solution with the V-cut guide plate.

3. Methodology and Numerical Approach

The proposed approach has been numerically investigated and verified using the model based on the standard heat sink I71 [15] (overall dimensions: W130.4mm x H57mm x L310mm). The model was built using the dimensions of the standard heat sink excluding the heat sink bottom base. The bottom base was removed in order to represent the heat sink model in a

classical way – the upper base and fins attached in parallel. The heat sink is equipped with 3 power IGBT modules CM400T-24S1 [16] (dimensions of the heat-producing area: W115mm x L82mm). The IGBT modules are installed on the top of the heat sink base in one row and represent a three-phase voltage source inverter for an ac electric drive. The power loss is assumed to be the same in each IGBT module. The range of power selected for the model investigation is from 50W to 100W in each module. A guide plate having a V-cut was attached to the bottom of the heat sink model. A benchmark model has a guide plate without V-cut to obtain the reference values corresponding to a conventional application of the heat sink.

A very common installation of the fans produced forced airflow through a heat sink is by the air inlet. Fans blow cool air into the fin area of the heat sink ensuring force air convection. However, in the proposed solution the air is extracted from the heat sink air outlet. For the numerical analysis, the velocity of air at the outlet is selected at 5m/s following the heat sink manufacture recommendations [15].

3.1 Numerical Modelling

The numerical study was performed using ANSYS 2021 R2 Workbench Package. The three-dimensional models are generated using ANSYS DesignModeler and transferred to ANSYS Meshing. The flow condition was determined by calculating the Reynolds number.

$$\mathrm{Re}_L = \frac{\rho u L}{\mu} \tag{1}$$

where ρ is density; u is velocity; L is the length of a heat sink; μ is kinematic viscosity.

Based on the Reynolds number exceeding 2300, the solver ANSYS FLUENT was used employing the k-epsilon turbulence model, accompanied by the following governing equations:

The continuity equation:

$$\nabla \cdot (\rho u) = 0 \tag{2}$$

where ∇ is gradient.

The momentum equation:

$$\nabla \cdot (\rho u u) = -\nabla p + \mu \nabla^2 u \tag{3}$$

where p is pressure.

The energy equation for the fluid domain:

$$\nabla \cdot \left(\rho u C_p T \right) = k \nabla^2 T \tag{4}$$

where C_p is specific heat capacity; T is temperature; k is thermal conductivity.

The energy equation for the solid domain:

$$\nabla^2 T = 0 \tag{5}$$

The surface heat flux is specified:

$$-k \left. \frac{dT}{dx} \right|_{x=0} = q \tag{6}$$

where q is the local heat flux density at the surface; $\frac{dT}{dx}$ is the temperature gradient.

The convection at the surface is specified:

$$-k \left. \frac{dT}{dx} \right|_{x=0} = h \left[T_\infty - T\left(x = 0, t \right) \right] \tag{7}$$

where h is the heat transfer coefficient; T_∞ is the fluid temperature.

The symmetry condition is specified:

$$-k \left. \frac{dT}{dx} \right|_{x=C_L} = 0 \tag{8}$$

where C_L is the centre line.

All numerical simulations have been carried out on a custom-built Workstation utilising an AMD Ryzen 9 5950X 16-Core processor equipped with 128GB RAM.

3.2 Domain Generation and Boundary Conditions

The schematic drawing of the three-dimensional model with dimension parameters are presented in Fig. 2 and Table 1, respectively. The symmetrical model was generated with the V-cut length as a parametric function. The symmetrical representation of the model offers the possibility of investigating just one section which significantly reduces the computational time of the ANSYS Fluent solver.

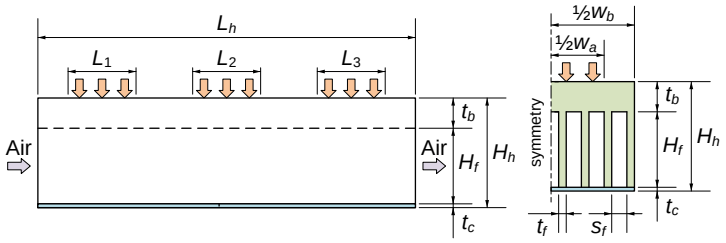

(a) (b)

Fig. 2. Schematic drawings of the model with the dimension parameters; (a) the heat sink model side view; (b) the heat sink model front view. The numerical model dimensions are given in Table 1.

Table 1. Numerical model dimensions (Fig. 2).

Symbol	Type	Value
L_h	heat sink length	310 mm
L_1; L_2; L_3	IGBT-Module length	82 mm
H_h	heat sink height	62 mm
H_f	fin height	47 mm
t_b	top base thickness	14 mm
t_c	guide plate thickness	1 mm
w_b	heat sink width	130.4 mm
w_a	IGBT-Module width	115 mm
t_f	fin thickness	1.4 mm
s_f	fin spacing	7.2 mm

The following boundary conditions are employed on the numerical model, presented in Fig. 3:

- Heat Sink (Solid): - Aluminium properties are assigned.
- Air Flow Region (Fluid): - Air properties are assigned.
- IGBT Modules (Wall): - Heat flux is applied to each IGBT module surface.
- Domain Central Faces (Symmetry): - Symmetry is assigned for all solid/fluid surfaces.
- Heat Sink Surrounding Faces (Wall): - Heat transfer to surrounding atmosphere by convection.
- Air Inlet (Pressure Inlet): - Air enters the heat sink at atmospheric pressure.

- Air Outlet (Velocity Outlet): - Air is extracted from the heat sink with 5 m/s in the positive *x*-direction according to the geometry.

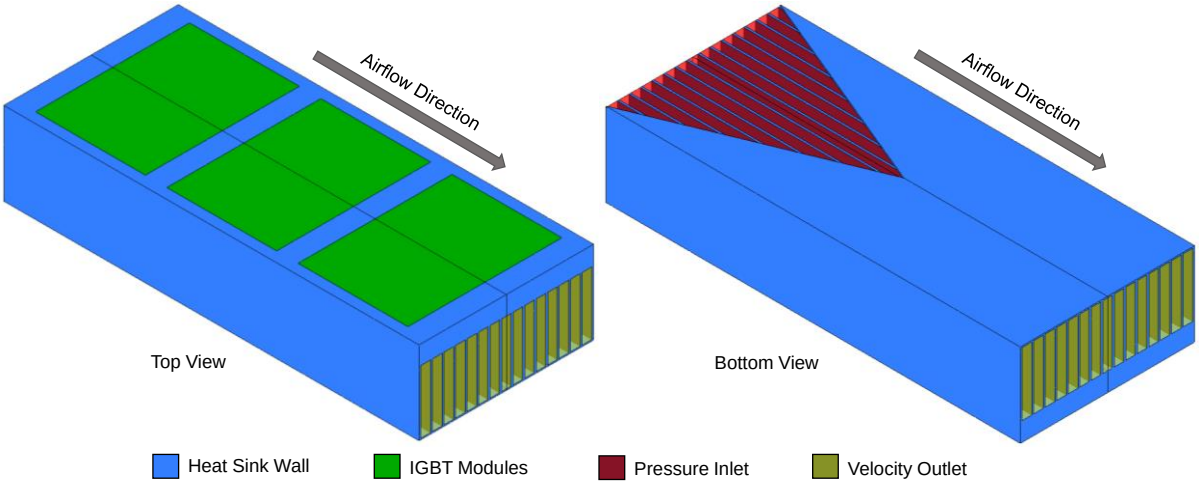

(a) (b)

Fig. 3. Schematic representation of (a) top and (b) bottom view of the numerical model with assigned boundary conditions.

3.4 ANSYS FLUENT Solver Settings

A double precision pressure-based solver was employed for all simulations and a coupled algorithm was defined for the pressure velocity coupling. A least-square cell based was specified for gradient, with second order momentum set for pressure. The turbulent kinetic energy and dissipation rate employed a first order upwind, and a second order upwind for momentum and energy. The absolute convergence criteria for all respective equation residual values are set to 10^{-6}. The material properties for aluminium have been defined according to Fischer *et al*. [17]. Convection was applied to all other surfaces with a coefficient based on Mueller *et al*. [18] and the ambient temperature was set to 24.85°C, respectively.

3.5 Mesh Sensitivity Study

A crucial step to obtain appropriate results is mesh generation. Therefore, a mesh sensitivity study was carried out on the benchmark model for the heat flux of 100W. A total of seven mesh models was simulated with a global element size ranging from 5 ~ 2 mm. The solid domain employed a tetrahedron mesh algorithm with a boundary layer applied to the upper surface of the heat sink due to the heat transfer and temperature gradient. Boundary layers are also assigned to the air channel walls to ensure solid to fluid heat transfer coefficients are

captured. The fluid domains are assigned with hexahedron mesh. For the fluid and solid domain, a structured and non-structured mesh was applied, respectively. Fig. 4 shows the front view of the meshed numerical model.

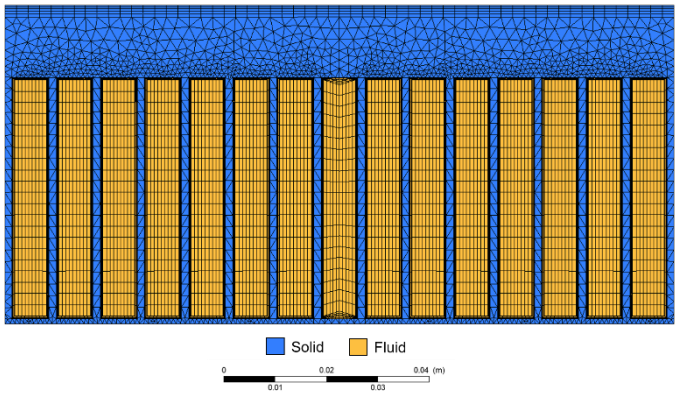

Fig. 4. Front view of the meshed numerical model.

The results of the mesh sensitivity study are shown in Table 2. The average surface temperatures of IGBT modules are stabilising around 653056 elements (M5). The average net surface temperature differences are compared against M6 (885884 elements) in Fig. 5, where the temperature variation between M5 to M7 was under 0.005%. Therefore, M6 (885884 elements) was determined as the best suited mesh configuration for this study and used for the simulations performed.

Table 2. Results of average surface IGBT module temperatures for mesh sensitivity study.

Mesh Model	No. of Elements	IGBT-1 [°C]	IGBT-2 [°C]	IGBT-3 [°C]
M1	153039	58.88	62.79	64.14
M2	186559	58.90	62.90	64.27
M3	232132	58.96	63.23	64.32
M4	365325	59.40	63.23	64.54
M5	653056	59.41	63.25	64.63
M6	885884	59.44	63.26	64.65
M7	1120902	59.44	63.27	64.67

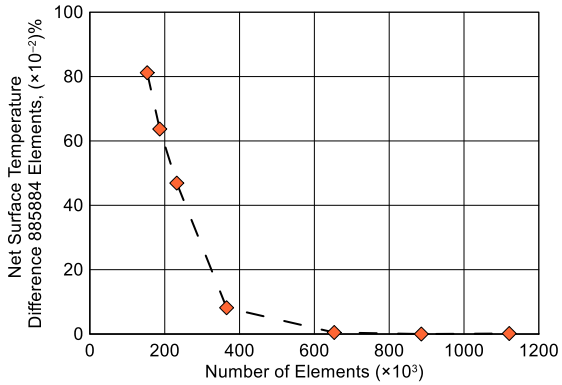

Fig. 5. Results of mesh sensitivity simulation where each IGBT module produces 100W of power loss.

4. V-cut Parametric Study

Fig. 6 demonstrates the installation of IGBT modules on the heat sink. It can be seen that the guide plate having a V-cut is attached to the bottom side of the heat sink. This model was numerically investigated under various lengths of V-cut *l* (mm). However, for the purpose of the extension of the results to the other cooling configuration the length of V-cut, as shown in Fig. 6, is expressed using a per unit parameter λ.

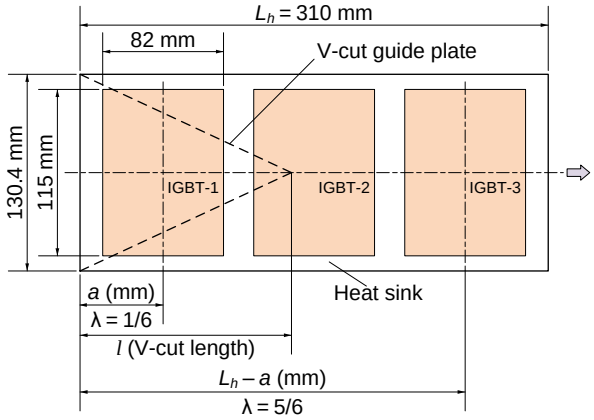

Fig. 6. Top view of a schematic drawing of the model for parametric study; the colour sections represent the location of individual IGBT modules.

The introduction of parameter λ provides an opportunity to apply the results to other similar heat sinks having different form factors. Also, the parameter λ reflects the fact that allocation of the installed power semiconductor modules can be varied in different applications. The parameter λ is developed using the assumptions that the module IGBT-2 is always located in the middle of the heat sink and the other modules (IGBT-1 and IGBT-3) are installed

symmetrically in respect to the module IGBT-2. Therefore, the middle of the IGBT-2 is pointed at 1/2 of the heat sink length L_h (1/2L_h = 155 mm; λ = 1/2 pu). Fig. 6 shows that the length between the edge of the heat sink and the centre of IGBT-1 is expressed as a (mm). If the centre of the modules IGBT-1 and IGBT-3 is installed exactly at 1/6 (5/6) of the total heat sink length L_h (a = 1/6L_h) then the length of the V-cut l (mm) is proportional to λ (pu) as $l = L_h\lambda$. However, if the length between the edge of the heat sink and the centre of the modules IGBT-1 and IGBT-3 is longer (a > 1/6L_h) or shorter (a < 1/6L_h) than 1/6L_h, the actual V-cut length in mm can be found as follows:

$$\begin{cases} l = 6a\lambda & 0 \le \lambda \le \dfrac{1}{6} \\ l = \dfrac{3}{2}\left(L_h - 2a\right)\lambda - \dfrac{1}{4}\left(L_h - 6a\right) & \dfrac{1}{6} \le \lambda \le \dfrac{5}{6} \\ l = 6a\lambda + L_h - 6a & \dfrac{5}{6} \le \lambda \le 1 \end{cases} \tag{9}$$

Fig. 7 illustrates the relation of the V-cut length (in mm) and the parameter λ (pu) for three different installations of the IGBT modules on the top of the heat sink used for analysis (Table 1). The graphs are drawn according to equation (9). The red line shows the relation V-cut length vs. λ for the case where the centre of IGBT-1 is located exactly at 1/6 of the total heat sink length (a = 51.67 mm; λ = 1/6). This IGBT modules' installation is implemented in the model applied for the numerical analysis. The blue line is related to the installation of IGBT-1 very close to the heat sink edge (a = 41 mm; λ = 1/6) whereas the green line is corresponding to the installation of IGBT-1 close to the middle module IGBT-2 (a = 73 mm; λ = 1/6). It demonstrates that the allocation of IGBT-1 is different in terms of length a (mm) but exactly the same in terms of parameter λ (pu). Therefore, the length of V-cut expressed in per unit can be applicable to the analysis of other heat sinks.

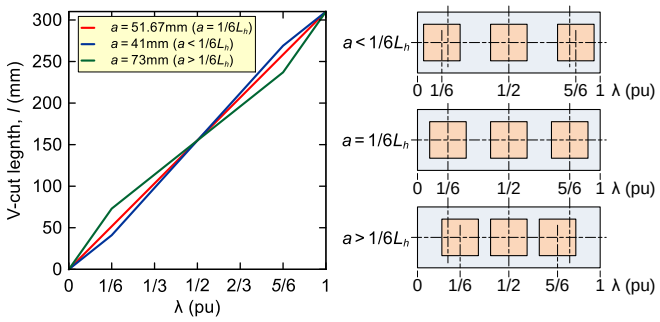

Fig. 7. V-cut length (mm) vs. parameter λ (pu) and illustration of the three different options to install the power modules on the top of the heat sink.

According to the study objective, the implementation of V-cut should provide a uniform distribution of the temperatures across the IGBT modules. At a particular, optimum value of the V-cut length, the average temperatures of the modules should be the same whereas the modules' temperature difference is negligible. Therefore, the criterion of the optimum length finding (expressed in per unit as the parameter λ) is formulated as follows:

$$\min \sum_{i=1}^{m} \left| T_i - T^* \right| \rightarrow \lambda_{OPT} \tag{10}$$

where $T^* = \frac{1}{m} \sum_{i=1}^{m} T_i$ is the average temperature of *m* semiconductor modules installed on the heat sink; T_i is the average surface temperature of *i*-th semiconductor module; *m* is the number of the semiconductor modules, *m* = 3 for this study (majority of three-phase power electronic converters have 3 semiconductor modules, however, in some applications the number of the modules can be *m* = 6).

5. Results and Discussion

Initially, the numerical analysis was applied to investigate the benchmark model having no V-cut (the parameter λ = 0). Fig. 8 shows the simulation results obtained for the benchmark model under three different levels of power loss per IGBT module: 50W, 80W, and 100W. It can be seen that the base of the heat sink has a significant temperature gradient due to non-uniform temperature distribution. The results of the benchmark model investigation as the reference value are given in Table 3.

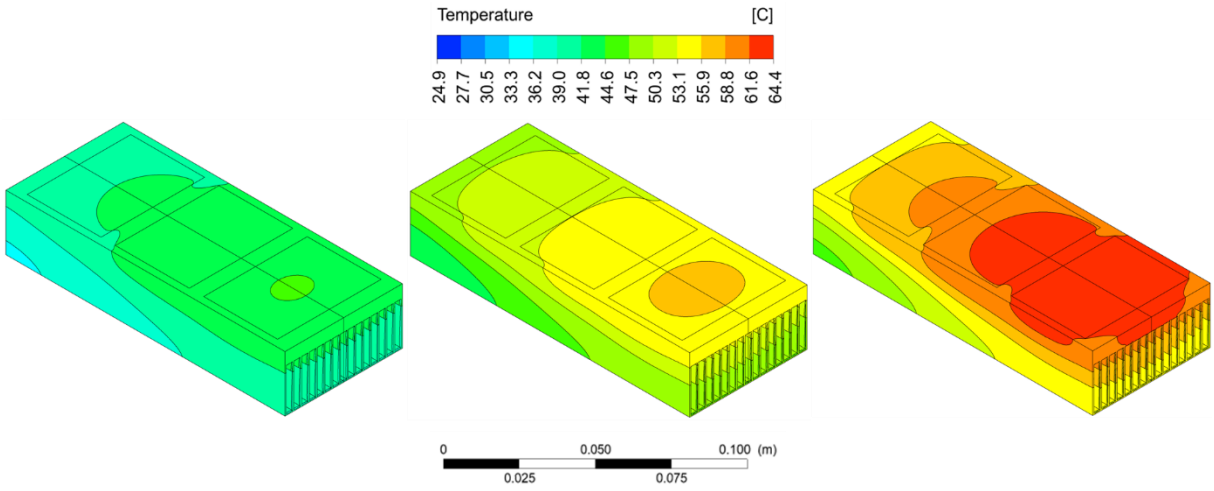

(a) (b) (c)

Fig. 8. Benchmark model temperature distribution: (a) 50W per IGBT module; (b) 80W per IGBT module; (c) 100W per IGBT module.

At the next stage, the thermal model of the heat sink was studied for 6 different V-cut lengths (λ = 0.19pu; λ = 0.32pu; λ = 0.45pu; λ = 0.58pu; λ = 0.71pu; λ = 0.84pu). The plots in Fig. 9 show the average surface temperature for individual IGBT modules vs. V-cut length λ in p.u. for the three different heat flux per IGBT module: 50W, 80W, and 100W. The plots demonstrate that the IGBT temperature distribution depends on the length of the V-cut where the optimum length is between λ = 0.45pu and λ = 0.58pu. To provide detailed analysis, further six V-cut lengths were studied to determine the optimum length (λ = 0.47pu; λ = 0.49pu; λ = 0.51pu; λ = 0.53pu; λ = 0.54pu; λ = 0.56pu) as shown in Fig. 10.

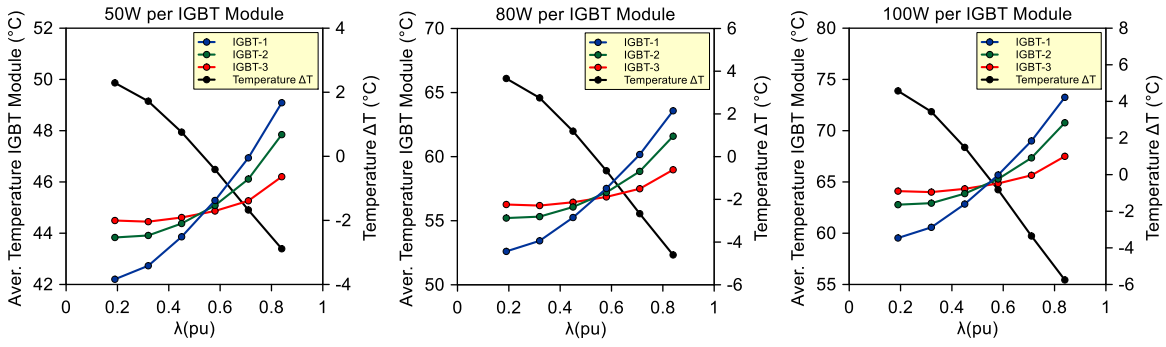

(a) (b) (c)

Fig. 9. Average surface temperature for individual IGBT modules and the temperature difference ΔT vs. V-cut length λ in p.u. for the heat flux per IGBT module (a) 50W, (b) 80W, (c) 100W.

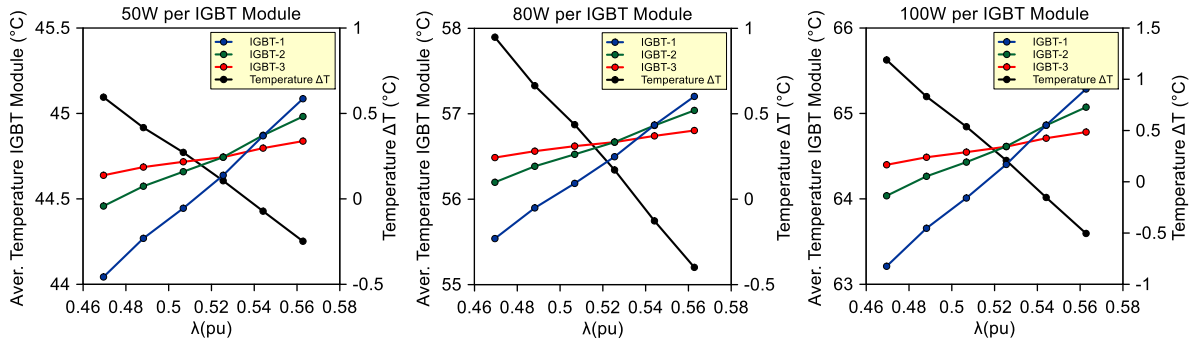

(a) (b) (c)

Fig. 10. Detailed analysis of the average surface temperature for individual IGBT modules and the temperature difference ΔT vs. V-cut length for the range of λ = 0.47-0.56pu; the heat flux per IGBT module (a) 50W, (b) 80W, (c) 100W.

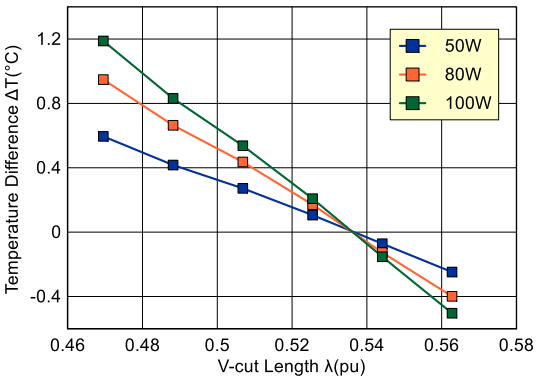

Fig. 11. Temperature difference ΔT vs. V-cut length λ in p.u. for the heat flux per IGBT module (a) 50W, (b) 80W, (c) 100W.

The results of the temperature difference ΔT vs. V-cut length for different heat fluxes are summarised in Fig. 11. It highlights that the optimum V-cut length to be λ ≈ 0.535pu.

The installation of the guide panel with the optimum V-cut length ensures equal temperature distribution. Fig. 9 demonstrates that the reduction of V-cut ($\lambda < \lambda_{OPT}$) decreases the temperature of the modules IGBT-1 and IGBT-2 and brings disbalance in the semiconductor temperatures. However, it will not produce a catastrophic failure of the IGBTs in contrast to the V-cut increase over the optimum value ($\lambda > \lambda_{OPT}$) where IGBT-1 could be extremely overheated and damaged.

The simulation results for the V-cut length λ = 0.53pu (most close to the optimum value) are shown in Fig. 12 for the same level of power loss in the IGBT modules as in the benchmark model. The temperature on the surface of the heat sink base is uniformed considerably better than in the benchmark model. It can be seen that the average temperatures

of IGBT modules are approximately the same and the temperature gradient in the areas where the IGBT modules are attached is significantly improved.

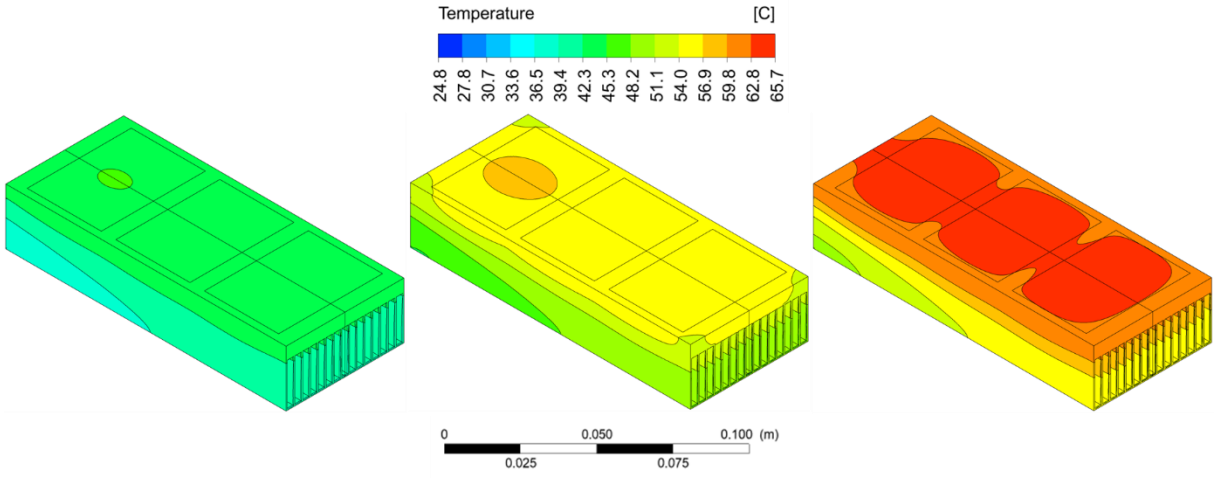

(a) (b) (c)

Fig. 12. Temperature distribution in the model having V-cut λ=0.53pu: (a) 50W per IGBT module; (b) 80W per IGBT module; (c) 100W per IGBT module.

Table 3. Comparison of the benchmark heat sink model (no V-cut) and the V-cut model (λ = 0.53pu).

Heat Flux per IGBT module (W)	Average Surface Temperature (°C) λ = 0				Average Surface Temperature (°C) λ = 0.53pu			
	IGBT-1	IGBT-2	IGBT-3	ΔT	IGBT-1	IGBT-2	IGBT-3	ΔT
50	42.15	44.05	44.74	2.60	44.64	44.75	44.75	0.11
60	45.60	47.89	48.72	3.11	48.59	48.72	48.72	0.13
70	49.06	51.73	52.69	3.63	52.54	52.69	52.69	0.15
80	52.53	55.58	56.67	4.15	56.50	56.67	56.67	0.17
90	55.98	59.41	60.65	4.67	60.45	60.64	60.64	0.19
100	59.44	63.25	64.63	5.19	64.40	64.61	64.61	0.21

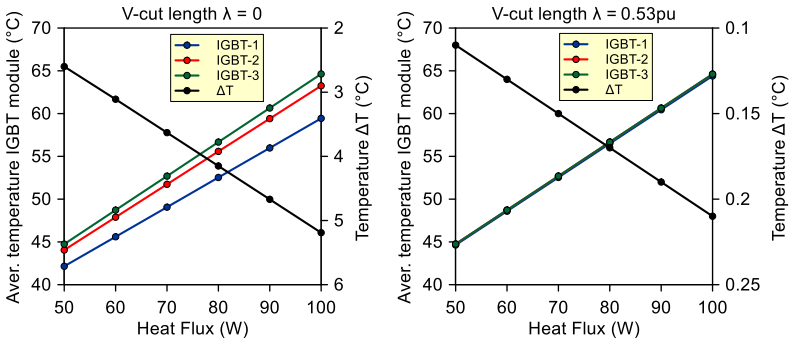

(a) (b)

Fig. 13. Distribution of the temperature across IGBT modules and temperature difference ΔT vs. heat flux per IGBT module for (a) benchmark model (no V-cut, λ = 0) and (b) model having V-cut λ = 0.53pu.

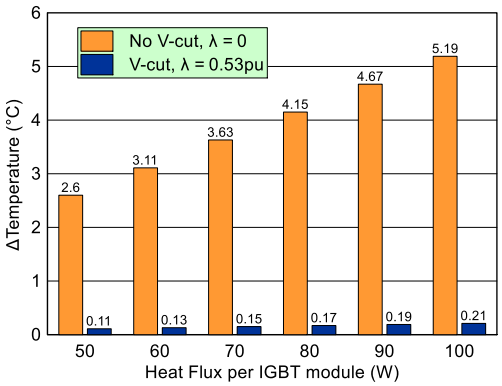

Fig. 14. Performance evaluation of the heat sink with V-cut (λ = 0.53pu) and without V-cut (λ = 0); the temperature difference ΔT vs. heat flux per IGBT module.

Table 3 demonstrates the simulation results for λ = 0.53 and its comparison with the reference values. The table results are graphically illustrated in Fig. 13 and Fig. 14. Fig. 13 shows the distribution of the temperature across IGBT modules and temperature difference ΔT vs. heat flux per IGBT module for the benchmark model (no V-cut, λ = 0) and the model having V-cut close to the optimum value (λ = 0.53pu). Fig 14 displays the performance evaluation of the heat sink without V-cut (λ = 0) and with V-cut (λ = 0.53pu) in terms of the temperature difference ΔT vs. heat flux per IGBT module. The temperature difference ΔT is an indirect parameter evaluating the temperature gradient across the heat sink surface. It demonstrates that the V-cut introduction is an effective solution to uniformly distribute the temperature in the IGBT modules and significantly reduce the temperature gradient of the module surfaces.

The length of V-cut affects the pressure drop ΔP of the airflow across the heat sink. Fig. 15 shows the correlation of ΔP with the V-cut length λ. With the V-cut length of λ = 0.53pu (close to the optimum value), a ΔP of 43.89 Pa was found compared to 20.17 Pa when λ = 0.

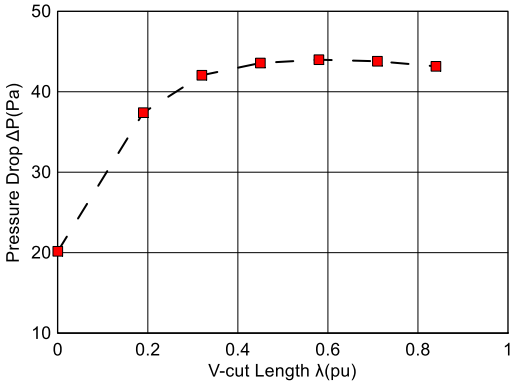

Fig. 15. Pressure drop (ΔP) across the heat sink for various V-cut lengths

Fig. 16 and Fig. 17 show the contours of velocity and static pressure for V-cut lengths λ = 0, λ = 0.53pu, and λ = 0.84pu. With a V-cut length of λ = 0, the average velocity magnitude across the heat sink is around 5.3 m/s, with the introduction of a V-cut on the bottom base plate, the velocity magnitude reduces considerably by drawing in more air. With a V-cut length of λ = 0.53pu, we can observe much larger velocities located under IGBT-2 and IGBT-3, due to vortex generation caused by the V-cut. This balance of higher-lower velocity distribution across the heatsink allows temperatures to be more homogeneous.

With active extraction located on the heatsink outlet, the negative static pressure distribution is observed from numerical simulations. With V-cut lengths greater than λ = 0.53pu, the parts of the fins located under IGBT-1 and IGBT-2 are more exposed to the atmosphere, resulting in natural convection rather than forced convection. This is clearly visible from the reduced incoming velocity under the respective IGBT modules, having a reverse effect on thermal distribution across the heatsink top surface.

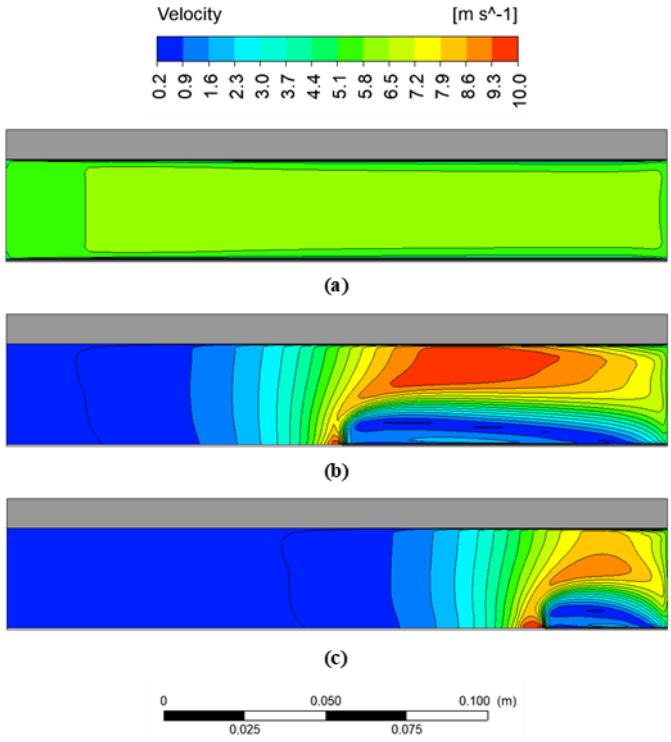

Fig. 16. Contours of velocity magnitude for V-cut lengths (a) λ = 0pu, (b) λ = 0.53pu, and (c) λ = 0.84pu

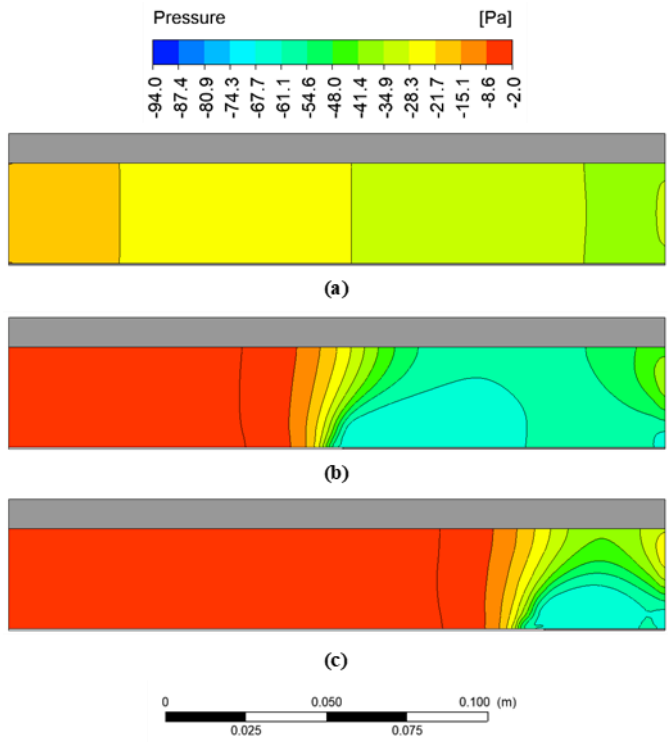

Fig. 17. Contours of static pressure for V-cut lengths (a) λ = 0pu, (b) λ = 0.53pu, and (c) λ = 0.84pu

5. Conclusion

This work discusses an approach to uniform the temperature distribution across three power semiconductor modules installed on the top of a conventional heat sink having parallel fins and operating under forced airflow. According to the approach, the conventional heat sink is equipped with a guide plate having a V-cut. The V-cut guide plate is attached to the bottom of the heat sink and provides redistribution of the airflow at the inlet to vary the heat transfer conditions over the heat sink length. This approach does not require modification of the heat sink and is considered as a very low-cost solution.

The thermal performance of the proposed heat sink was numerically investigated using Ansys software. The numerical model is based on a standard heat sink (type I71) with forced airflow at a constant speed of 5m/s applied to cool three IGBT modules (CM400ST-24S1) installed on the top. The model was analysed under steady-state conditions for various sizes of V-cut and power losses in the IGBT modules. The simulation results have shown that the optimum length of V-cut expressed in p.u. is approximately $\lambda \approx 0.535$pu. The heat sink performance has been analysed at the power loss of 100W in each IGBT module and V-cut length $\lambda = 0.53$pu. It has been shown that the difference in the average temperatures of the IGBT modules does not exceed 0.21°C. The parameter λ representing the V-cut dimensions is developed in terms of per unit and can be applied to the analyses of other similar configurated cooling systems having a different size or heat sink form factor.

The advantage of the uniform temperature distribution is the significant reduction in the temperature gradient across the semiconductor structures of the power modules. The uniform temperatures of the power semiconductors assembled in a three-phase power circuit ensure balanced/symmetrical operation of the external circuit and provide the equal load condition of the semiconductors. Hence, both the temperature gradient reduction and the uniform temperature distribution bring improvement in the power electronic modules' lifetime and reliability.

References

[1] J. Falck, C. Felgemacher, A. Rojko, M. Liserre and P. Zacharias, "Reliability of power electronic systems: An industry perspective," *IEEE Industrial Electronics Magazine*, vol. 12, no. 2, pp. 24-35, June 2018, doi: 10.1109/MIE.2018.2825481

[2] H. Wu, C. Ye, Y. Zhang, F. Hou and J. Nie, "Research on lifetime distribution and reliability of IGBT module based on accelerated life test and K-S test," *Int. Journal of*

Engineering Systems Modelling and Simulation, vol. 11, no. 1, pp. 1-10, 2019, doi: 10.1504/IJESMS.2019.098903

[3] S. Yang, A. Bryant, P. Mawby, D. Xiang, L. Ran and P. Tavner, "An industry-based survey of reliability in power electronic converters," *IEEE Trans. on Industry Applications,* vol. 47, no. 3, pp. 1441-1451, May-June 2011, doi: 10.1109/TIA.2011.2124436

[4] D. Christen, M. Stojadinovic and J. Biela, "Energy efficient heat sink design: Natural versus forced convection cooling," *IEEE Trans. on Power Electronics*, vol. 32, no. 11, pp. 8693-8704, Nov. 2017, doi: 10.1109/TPEL.2016.2640454

[5] B. Gao, F. Yang, M. Chen, L. Ran, I. Ullah, S. Xu, and P. Mawby, "A temperature gradient-based potential defects identification method for IGBT module," *IEEE Trans. on Power Electronics*, vol. 32, no. 3, pp. 2227-2242, March 2017, doi: 10.1109/TPEL.2016.2565701

[6] M. Andresen, and M. Liserre, "Impact of active thermal management on power electronics design," *Microelectronics Reliability,* vol. 54, nos. 9-10, pp. 1935-1939, Sept.-Oct. 2014, doi: 10.1016/j.microrel.2014.07.069

[7] A. Anuchin, V. Podzorova, V. Popova, I. Gulyaev, F. Briz and Y. Vagapov, "Model predictive torque control of a switched reluctance drive with heat dissipation balancing in a power converter," in *Proc. 60th IEEE Int. Scientific Conf. on Power and Electrical Engineering of Riga Technical University*, Riga, Latvia, 7-9 Oct. 2019, pp. 1-6, doi: 10.1109/RTUCON48111.2019.8982255

[8] A. Anuchin, F. Briz, I. Gulyaev, A. Zharkov, M. Gulyaeva, and V. Popova, "Heat dissipation balancing in a switched reluctance drive by combined use of active and passive thermal control methods," in *Proc. 20th Int. Symp. on Power Electronics*, Novi Sad, Serbia, 23-26 Oct. 2019, pp. 1-5, doi: 10.1109/PEE.2019.8923285

[9] Z. Khattak, and H.M. Ali, "Air cooled heat sink geometries subjected to forced flow: A critical review," *International Journal of Heat and Mass Transfer,* vol. 130, pp. 141-161, March 2019, doi: 10.1016/j.ijheatmasstransfer.2018.08.048

[10] C.-H. Huang, and Y.-H. Chen, "An optimal design problem in determining non-uniform fin heights and widths for an impingement heat sink module," *Applied Thermal Engineering*, vol. 63, no. 2, pp. 481-494, Feb. 2014, doi: 10.1016/j.applthermaleng.2013.11.008

[11] C.-H. Huang, and Y.-H. Chen, "An impingement heat sink module design problem in determining simultaneously the optimal non-uniform fin widths and heights,"

International Journal of Heat and Mass Transfer, vol. 73, pp. 627-633, June 2014, doi: 10.1016/j.ijheatmasstransfer.2014.02.026

[12] X. Wang, W. Zhang, H. Liu, L. Chen, and Z. Li, "Numerical simulation on variable width multi-channels heat sinks with non-uniform heat source," in *Proc. Int. Conf. on Electronic Packaging Technology and High Density Packaging*, Beijing, China, 10-13 Aug. 2009, pp. 1155-1158, doi: 10.1109/ICEPT.2009.5270609

[13] B.B. Al-Khamaiseh, M. Razavi, Y.S. Muzychka, and S. Kocabiyik, "Thermal resistance of a 3-D flux channel with nonuniform heat convection in the sink plane," *IEEE Trans. on Components, Packaging and Manufacturing Technology*, vol. 8, no. 5, pp. 830-839, May 2018, doi: 10.1109/TCPMT.2017.2776601

[14] M.L. Elsayed, O. Mesalhy, R.H. Mohammed, J.P. Kizito, Q.H. Leland, and L.C. Chow, "Enhancement of a heat sink performance using a partial shield and/or a guide plate," *International Journal of Heat and Mass Transfer*, vol. 134, pp. 948-958, May 2019, doi: 10.1016/j.ijheatmasstransfer.2019.01.096

[15] Tecnoal, "I71 heat sink data sheet," [Online]. Available: http://www.tecnoal.it/media/7747/i71.pdf.

[16] Mitsubishi Electronics, „IGBT Moudule S1 series CM400ST-24S1," [Online]. Available: https://www.mitsubishielectric.com/semiconductors/content/product/powermodule/igbt/s1_series/cm400st-24s1_e.pdf

[17] U. Fischer, M. Heinzler, F. Näher, H. Paetzold, R. Gomeringer, R. Kilgus, S. Oesterle and A. Stephan, *Tabellenbuch Metall*, vol. 44. Europa Lehrmittel: Haan-Gruiten, Germany, 2008.

[18] A. Mueller, C. Buennagel, S. Monir, A. Sharp, Y. Vagapov, and A. Anuchin, "Numerical design and optimisation of a novel heatsink using ANSYS steady-state thermal analysis," in *Proc. 27th Int. Workshop on Electric Drives*, Moscow, Russia, 27-30 Jan. 2020, pp. 1-5, doi: 10.1109/IWED48848.2020.9069568